Analysis of the Properties of the N-Terminal Nucleotide-Binding Domain of Human P-Glycoprotein†

Catherine L. Booth,‡ Lukasz Pulaski,§ Michael M. Gottesman,§ and Ira Pastan*,‡

Laboratories of Molecular Biology and Cell Biology, National Cancer Institute, National Institutes of Health, Bethesda, Maryland 20892

Received December 22, 1999; Revised Manuscript Received February 28, 2000

ABSTRACT: Human P-glycoprotein, the *MDR*1 gene product, requires both Mg^{2+}-ATP binding and hydrolysis to function as a drug transporter; however, the mechanism(s) defining these events is not understood. In the present study, we explored the nature of Mg^{2+}-ATP binding in the N-terminal nucleotide-binding domain of human P-glycoprotein and identified the minimal functional unit required for specific ATP binding. Recombinant proteins encompassing amino acids within the region beginning at 348 and ending at 707 were expressed in *Escherichia coli*, purified from inclusion bodies under denaturing conditions, and renatured by rapid dilution. The ability of ATP to interact with these proteins was examined by use of the photoactive ATP analogue [α-^{32}P]-8-azido-ATP. Photoaffinity labeling of recombinant proteins identified the region between amino acids 375 and 635 as the region necessary to obtain specific ATP-binding properties. Specific protein labeling was saturable, enhanced by Mg^{2+}, and inhibited by ATP. Recombinant proteins confined within the region beginning at amino acid 392 and ending at amino acid 590 demonstrated nonspecific [α-^{32}P]-8-azido-ATP labeling. Nonspecific labeling was not enhanced by Mg^{2+} and was inhibited only by high concentrations of ATP. Using a D555N mutated protein, we found that the conserved aspartate residue in the Walker B motif plays a role in magnesium-enhanced ATP-binding. Taken together, these data define the region of the N-terminal nucleotide-binding domain of P-glycoprotein that is required for specific ATP binding and suggest that magnesium may play a role in stabilizing the ATP-binding site.

Multidrug resistance is a major obstacle in the effective treatment of cancer by chemotherapeutic agents. Regardless of whether multidrug resistance of tumor cells is intrinsic or acquired after exposure to cytotoxic agents such as epipodophyllotoxins, anthracyclines, vinca alkaloids, or taxol, therapeutic failure frequently is observed. In part, phenotypic multidrug resistance is due to the *MDR*1 gene product, P-glycoprotein, which is found in several tissues throughout the body and is overexpressed in many cancers (*1*, *2*).

The human *MDR*1 cDNA encodes 1280 amino acid residues resulting in a 170-kDa plasma membrane glycoprotein. Sequence analysis indicates that P-glycoprotein is composed of 12 transmembrane domains in two homologous halves connected by a linker peptide. Each half of P-glycoprotein contains six transmembrane regions and one cytoplasmic nucleotide-binding domain (NBD)[1] with characteristic Walker A and B motifs (*3*). P-Glycoprotein is a member of the family of ATP-binding cassette (ABC) transporters and acts as an ATP-dependent efflux pump that extrudes anticancer drugs from the cell, thereby decreasing intracellular drug concentrations. Both Mg^{2+}-ATP binding and hydrolysis are necessary for P-glycoprotein function (*4*); however, the mechanism(s) defining these events is not precisely understood. The purification and reconstitution of P-glycoprotein in the presence of lipids provides a model system to study these mechanism(s) (*5*) but is limited by the low yield of purified protein obtained.

Expression and purification of soluble NBDs of various ABC transporters has been reported (*6*−*10*). Several recombinant proteins containing N-terminal and C-terminal NBDs derived from P-glycoprotein also have been expressed (*11*−*16*) and have enabled the investigation of nucleotide binding in these protein regions. However, characterization of the NBD in these regions was achieved primarily by fluorescence-based analysis with TNP-ATP or MANT-ATP as probes. Comparison of data obtained from fluorescence assays with soluble recombinant protein to that of the full-length protein is compromised by interference from lipids necessary for stable reconstitution of the full-length protein. Additionally, fluorescence of TNP-ATP is quenched by the presence of

† C.L.B. was supported in part by the National Institute of General Medical Sciences Pharmacology Research Associate Program.

* To whom correspondence should be addressed, at the Laboratory of Molecular Biology, Building 37, Room 4E16, National Cancer Institute, National Institutes of Health, 37 Convent Dr. MSC 4255, Bethesda, MD 20892-4255. Telephone 301-496-4797. FAX 301-402-1344; E-mail pasta@helix.nih.gov.

‡ Laboratory of Molecular Biology.

§ Laboratory of Cell Biology.

[1] Abbreviations: NBD, nucleotide-binding domain; ABC, adenosine triphosphate- (ATP-) binding cassette; TNP-ATP, 2′,3′-*O*-(2,4,6-trinitrophenyl)adenosine triphosphate; MANT-ATP, 2′(3′)-*N*-methylanthraniloyladenosine triphosphate; 8-azido-ATP, 8-azidoadenosine-5′-triphosphate; NBD1, N-terminal nucleotide-binding domain; IPTG, isopropyl β-D-thiogalactoside; CD, circular dichroism; CFTR, cystic fibrosis transmembrane conductance regulator.

10.1021/bi992931x
Published on Web 04/13/2000

Table 1: Cloning Summary for Expression Vectors

plasmid name	cloning vector	PCR primers (5′ → 3′)[a]	restriction enzymes[b]
pET-NBD1*MDR*1-C431A (358−707)	pET3a	A: GCAATACATATGGCAAGAGGAGCAGCTTATGAAATCTTC	A: *Nde*I
		B: AAAGGATCCTCATTCAGTTAAATTTAGCTTCATAATCCT	B: *Bam*HI
pET-NBD1*MDR*1-C431A/D555N (358−707)	pET3a	A: GCAATACATATGGCAAGAGGAGCAGCTTATGAAATCTTC	A: *Nde*I
		B: AAAGGATCCTCATTCAGTTAAATTTAGCTTCATAATCCT	B: *Bam*HI
pET-NBD1*MDR*1-C431A (412−574)	pET23a	A: GTTAAGATGCATATGGGCCTGAACCTGAAGGTGCAGAGT	A: *Nde*I
		B: ACCTTTGAATTCTCAATCCAGAGCCACCTGAACCACTGC	B: *Eco*RI
pET-NBD1*MDR*1-C431A (358−590)	pET3a	A: GCAATACATATGGCAAGAGGAGCAGCTTATGAAATCTTC	A: *Nde*I
		B: ATTGGATCCTCAAGACAAACGATGAGCTATCACAATGGT	B: *Bam*HI
pET-NBD1*MDR*1-C431A (358−635)	pET23a	A: GAGATATACATATGGCAAGAGGAGCA	A: *Nde*I
		B: TCTCCTCGAGCTAAACTTCATTTCCTGCTGTCTG	B: *Xho*I
pET-NBD1*MDR*1-C431A (409−635)	pET23a	A: GAGACATATGATCTTGAAGGGCCTGAACCTG	A: *Nde*I
		B: TCTCCTCGAGCTAAACTTCATTTCCTGCTGTCTG	B: *Xho*I
pET-NBD1*MDR*1-C431A (375−707)	pET23a	A: GAGACATATGATTGACAGCTATTCGAAGAGT	A: *Nde*I
		B: TCTCCTCGAGCTATTCAGTTAAATTTAGCTTCAT	B: *Xho*I
pET-NBD1*MDR*1-C431A (392−707)	pET23a	A: GAGACATATGTTGGAATTCAGAAATGTTCAC	A: *Nde*I
		B: TCTCCTCGAGCTATTCAGTTAAATTTAGCTTCAT	B: *Xho*I
pET-NBD1*MDR*1-C431A (348−635)	pET23a	A: GAGACATATGGCATCTCCAAGCATTGAAGCATTTGCAAAT-GCAAGAGGAGCAGCT	A: *Nde*I
		B: TCTCCTCGAGCTAAACTTCATTTCCTGCTGTCTG	B: *Xho*I

[a] A, forward primer; B, reverse primer. [b] A, N-terminal; B: C-terminal.

various cations, including magnesium (*17*, *18*), thus hindering the evaluation of magnesium-dependent process. In contrast, the photoactive ATP analogue [α-^{32}P]-8-azidoadenosine 5′-triphosphate ([α-^{32}P]-8-azido-ATP), has been used extensively to examine various biochemical questions relating to the ATP-binding properties of many proteins (*19*−*23*).

The first use of [α-^{32}P]-8-azido-ATP to characterize nucleotide-binding properties of P-glycoprotein was reported by Cornwell et al. (*24*) using membrane vesicles prepared from a highly multidrug-resistant cell line (KB-V1). Most recently, our laboratory demonstrated the use of [α-^{32}P]-8-azido-ATP to characterize the kinetics of ATP binding to P-glycoprotein with membranes prepared from baculovirus and vaccinia virus expression systems (*25*). This work demonstrated that both NBDs are essential for proper function but that they are asymmetric (*25*). Moreover, this work suggested that in addition to complexing with ATP in the active site, magnesium might play an additional role in stabilizing the conformation of the active site or changing the overall transporter (*25*). Magnesium often plays an important role in the structure and function of various proteins (*26*−*28*).

In the present study, we explored the nature of Mg^{2+}-ATP binding in the N-terminal NBD of human P-glycoprotein (NBD1) and identified the minimal functional unit required for specific ATP binding by expressing NBD1 as a soluble recombinant protein and utilizing [α-^{32}P]-8-azido-ATP. It has been shown previously that the N-terminal NBD of human P-glycoprotein is labeled preferentially with [α-^{32}P]-8-azido-ATP under binding conditions and that a chimeric human P-glycoprotein molecule that contains two N-terminal ATP binding domains is expressed at the cell surface and is functional for transport (*25*). Thus, we chose to express NBD1 of human P-glycoprotein as a soluble recombinant protein in the present work. Through studying the nucleotide binding properties of NBD1 proteins of varying lengths, we determined that the minimal functional unit required for specific ATP binding was composed of amino acids 375−635. The highest ATP binding was obtained with a recombinant protein composed of amino acids 348−635.

EXPERIMENTAL PROCEDURES

Materials. pET-3a and pET-23a plasmid DNA were obtained from Novagen (Madison, WI). pTM1-*MDR*1 and pTM1-*MDR*1-D555N were supplied by Dr. Christine Hrycyna (*25*, *29*). Competent *Escherichia coli* (DH5α) and custom primers were purchased from Life Technologies (Gaithersburg, MD). Competent *E. coli* (BL21 λDE3) was prepared as described previously (*30*). All restriction enzymes were purchased from New England Biolabs (Beverly, MA). [α-^{32}P]-8-Azidoadenosine-5′-triphosphate (20 Ci/mmol) was purchased from ICN (Costa Mesa, CA).

Construction of Expression Vectors. Initially, the pTM1-*MDR*1 vector containing the *MDR*1 coding sequence was used as the template for construction of the expression vector encoding an *MDR*1 fragment encompassing amino acids 358−707. A coding sequence bp 1072−2121 fragment was obtained by PCR with coding (forward) and noncoding (reverse) primers as shown in Table 1. The purified reaction product was digested with *Nde*I and *Bam*HI. This fragment was incubated with alkaline phosphatase for 1 h at 37 °C to avoid self-ligation by removing free phosphate groups at the 5′ ends and subsequently cloned into the pET3a vector. The resulting expression vector was used as a template for site-directed mutagenesis to introduce a C431A mutation. Nucleotide mutations at positions 1291 (T → G) and 1292 (G → C) were achieved by sequence overlap PCR methodology. Two internal complementary primers were used, each containing the mutation of interest. The coding sequence for the C431A mutant primer was 5′-GTTGGAAACAGTG-GCGCTGGGAAGAGCACA-3′. These primers were used in conjunction with two outer primers that contained the unique restriction sites *Bst*BI (coding strand, 5′-TAAGC-CAAGTATTGACAGCTA-3′) and *Nco*I (noncoding strand, 5′-TGACAGCTTTCTCAATCTCAT-3′). The resulting fragment was digested with *Bst*BI and *Nco*I, incubated with alkaline phosphatase, and recloned into the pET3a-based vector obtained in the previous step. The plasmid obtained contained a sequence encoding *MDR*1 amino acids 358−707 with a C431A mutation and was labeled pET-NBD1*MDR*1-C431A (358−707). A plasmid, containing a

sequence encoding *MDR*1 amino acids 358−707 with both C431A and D555N mutations, was prepared as described above, with the pTM1-*MDR*1-D555N vector bearing the *MDR*1 coding sequence with a D555N mutation as the primary template, and was labeled pET-NBD1*MDR*1-C431A/D555N (358−707). pET-NBD1*MDR*1-C431A was used as the template for construction of subsequent expression vectors as indicated in Table 1. All constructs were sequenced fully in both directions by DNA sequencing using an Applied Biosystems Inc. 377 automated sequencer.

Expression and Purification of NBD Proteins. Purified plasmid was transformed into competent *E. coli* strain BL21 (λDE3) and grown overnight on LB agar containing 100 μg/mL ampicillin. Because the expressed nucleotide sequence contained several rare codons for which *E. coli* contains small amounts of tRNA, the expression was performed in cells transformed previously with the pUB500 plasmid containing a gene for the arginine tRNA recognizing the UCC anticodon (*30*). Superbroth (1 L) containing 2% glucose, 0.05% $MgSO_4$, and 100 μg/mL ampicillin was inoculated with the bacterial colonies. Expression of the recombinant protein was induced with 1 mM isopropyl β-D-thiogalactoside (final concentration) when OD_{600} reached a value of 3. The cells were harvested 90 min after induction by centrifugation at 3500 rpm for 30 min. Inclusion-body protein was washed by sequential resuspension and centrifugation at 13 000 rpm for 50 min in 200 mL of buffer containing 50 mM Tris and 20 mM EDTA, pH 8.0. The initial resuspension buffer contained 2.5% Triton X-100, followed by resuspension buffer containing 1% Triton X-100 and three additional washes in the absence of detergent. The final pellet was resuspended in 20 mL of buffer containing 50 mM Tris and 20 mM EDTA, pH 8.0, and centrifuged at 20 000 rpm for 20 min, and the pellet was stored at −70 °C. Inclusion body pellets were homogenized in solubilization buffer (6 M guanidine hydrochloride/0.1 M Tris, pH 8.0/2 mM EDTA) and stored at room temperature for at least 2 h. Solubilized inclusion-body protein was harvested by centrifugation at 20 000 for 30 min. Renaturation was initiated by a rapid 100-fold dilution of the solubilized protein into refolding buffer (0.1 M Tris, pH 8.0/0.5 M L-arginine/2 mM EDTA) and maintained at 10 °C for 12 h. Renatured protein was dialyzed against 20 mM Tris, pH 8.0/100 mM NaCl (50 L) overnight. Glycerol was added to the dialyzed protein (15% final concentration) and the protein was concentrated (∼500 μg/mL) by use of Centriprep10 concentrators (Amicon, Danvers, MA) and stored at 4 °C.

[α-^{32}P]-8-Azido-ATP Labeling. In 1.5 mL microcentrifuge tubes, NBD1 protein (∼300 μg/mL in 20 mM Tris-HCl, pH 8.0/100 mM NaCl/15% glycerol) in the absence or presence of $MgSO_4$ was incubated on ice for 3 min. Under subdued light conditions, [α-^{32}P]-8-azido-ATP (2.5 μCi) was added per tube and incubated for 10 min on ice. The tube contents were exposed to UV irradiation (365 nm; Black-Ray lamp, model XX-15, UVP, Uplard, CA) for 15 min on ice to facilitate cross-linking. After addition of SDS−PAGE sample loading buffer to the tube, the tube contents were vortex-mixed and stored at room temperature for 30 min prior to analysis by SDS−polyacrylamide gel electrophoresis as previously described (*31*). Quantitation of radioactivity was achieved by phophorimage analysis (Storm 860; Molecular Dynamics, Sunnyvale, CA). In some experiments, various nucleotides were added to the reaction tube prior to the addition of [α-^{32}P]-8-azido-ATP in order to examine the effect of unlabeled nucleotides on [α-^{32}P]-8-azido-ATP labeling.

Measurement of ATPase Activity. P-Glycoprotein-associated ATPase activity of recombinant proteins was determined as the vanadate-sensitive release of inorganic phosphate from Mg^{2+}ATP as described (*32*). Protein solution (∼100 μg/mL) was incubated at 37 °C for 5 min in a reaction mixture containing 50 mM Tris (pH 7.5), 5 mM sodium azide, 2 mM EGTA (pH 7.0), 2 mM ouabain, 2 mM DTT, 50 mM KCl, and 10 mM $MgCl_2$. The reactions were then started by the addition of 5 mM ATP to the assay mixture (a total volume of 100 μL) and incubated at 37 °C for 20 min. Reactions were stopped by the addition of 100 μL of 5% SDS solution and the amount of inorganic phosphate liberated was measured by a colorimetric reaction (*33*). The vanadate-sensitive activities were calculated as the differences between the ATPase activities obtained in the absence and presence of 300 μM sodium orthovanadate.

Circular Dichroism. CD spectra were measured on a Jasco J-720 spectropolarimeter (Jasco, Tokyo). Sample consisted of NBD1 (358−707) or NBD1 D555N (358−707) proteins (∼250 μg/mL) in 50 mM potassium phosphate/50 mM NaCl (pH 7.0). CD spectra were measured in 1 mm path length quartz CD cuvettes, at 20 mdeg sensitivity, 0.5 nm resolution, and 1.0 nm bandwidth at a speed of 20 nm/min at a constant temperature of 20 °C. Temperature melt studies were performed by monitoring molar ellipticity at 220 nm over the temperature range of 20−80 °C at a rate of 1 °C/min. Protein secondary structure was determined from CD spectra by numerical decomposition with CDNN (Institut für Biotechnologie, Martin-Luther-Universitat, Halle-Wittenberg, Germany).

Size-Exclusion Chromatography. Recombinant NBD1 proteins (∼0.5 mg/mL) were eluted from a Superdex 200 high-resolution gel-filtration column (10 × 300 mm, 24 mL bed volume, Pharmacia Biotech, Piscataway, NJ) at a flow rate of 0.4 mL/min with 0.02 M Tris, pH 8.0, containing 0.1 M NaCl and 15% (w/v) glycerol. Absorbency of the column eluent was monitored continuously at 280 nm. A calibration curve was constructed from the elution profiles of proteins with known molecular weights that were analyzed under the same conditions described above. The predicted molecular weights of the recombinant proteins were determined from the calibration curve.

Data Analysis. The percentage inhibition of [α-^{32}P]-8-azido-ATP labeling of NBD protein was calculated as follows:

$$\%\ \text{inhibition} = \left(1 - \left[\frac{[^{32}\text{P}]\text{-8-azido-ATP labeling density} + \text{inhibitor}}{[^{32}\text{P}]\text{-8-azido-ATP labeling density} - \text{inhibitor}}\right]\right) \times 100$$

Inhibition constants, IC_{50} and % maximum inhibition, were estimated from the percentage inhibition of [α-^{32}P]-8-azido-ATP labeling versus inhibitor concentration data by nonlinear least-squares regression (WinNonlin; Statistical Consultants, Inc., Apex, NC) according to the standard Michaelis−Menten equation.

The kinetics of Mg^{2+}-enhanced [α-^{32}P]-8-azido-ATP labeling was determined from the amount of [α-^{32}P]-8-azido-

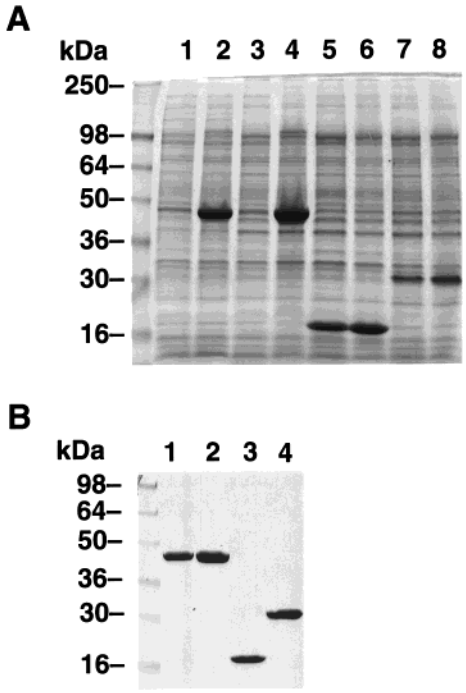

FIGURE 1: Expression and purification of NBD1 proteins. Protein fractions (10 μg of total protein/lane) were separated by SDS−PAGE and identified by colloidal blue staining (Novex, San Diego, CA). (A) Expression of NBD1 proteins before (lanes 1, 3, 5, and 7) and after (lanes 2, 4, 6, and 8) IPTG induction. NBD1 proteins were as follows: NBD1 (358−707), lanes 1−2; NBD1 D555N (358−707), lanes 3 and 4; NBD1 (412−574), lanes 5 and 6; and NBD1 (358−590), lanes 7 and 8. (B) Purified NBD1 proteins were identified by colloidal blue staining as follows: NBD1 (358−707), lane 1; NBD1 D555N (358−707), lane 2; NBD1 (412−574), lane 3; and NBD1 (358−590), lane 4.

ATP incorporation versus Mg^{2+} concentration data by nonlinear least-squares regression according to the standard sigmoidal E_{max} model.

RESULTS

Amino-Terminal Cytoplasmic Loop Containing the Nucleotide-Binding Domain of Human P-Glycoprotein Is Expressed in Escherichia coli and Retains the Ability To Bind ATP. Recombinant proteins, encompassing amino acids 412−574, 358−590, and 358−707 of human P-glycoprotein each with a C431A mutation, encoded by pET-NBD1*MDR*1-C431A-based plasmids (Table 1) were expressed and purified from *E. coli*, purified from inclusion bodies under denaturing conditions, and renatured by rapid dilution. The C431A mutant was used to prevent disulfide interactions. The vast majority of each protein was localized in inclusion bodies and was isolated by centrifugation from the homogenized bacteria. Solubilization of inclusion-body protein was achieved in buffer containing the strong denaturant guanidine hydrochloride. Expression and purification of the proteins is illustrated in Figure 1. Lanes 1, 3, 5, and 7 represent the total bacterial protein of each construct prior to induction (Figure 1A). After induction with IPTG, each protein was overexpressed and constituted the major component among total bacterial protein (lanes 2, 4, 6, and 8) (Figure 1A). Extensive washing of the inclusion body protein in the presence of detergent followed by renaturation and dialysis was sufficient to obtain highly purified recombinant proteins (Figure 1B).

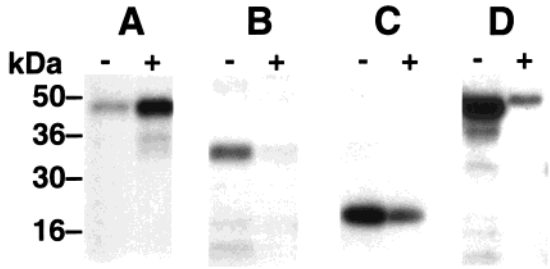

FIGURE 2: [α-^{32}P]-8-Azido-ATP labeling of NBD1 proteins. NBD1 proteins were photoaffinity-labeled with 2.5 μM [α-^{32}P]-8-azido-ATP in the absence (−) and presence (+) of 5 mM $MgSO_4$ and analyzed by SDS−PAGE and autoradiography. NBD1 proteins were as follows: (A) NBD1 (358−707), (B) NBD1 (358−590), (C) NBD1 (412−574), and (D) NBD1 D555N (358−707).

To determine if the recombinant proteins possessed the ability to bind ATP, the use of the photoactive ATP analogue [α-^{32}P]-8-azido-ATP was employed because the radiolabeled compound has been shown previously to label P-glycoprotein in a specific manner (*24*, *25*, *34*). In addition, 8-azido-ATP has been shown to be hydrolyzed by P-glycoprotein (*35*). In this experiment, recombinant proteins were incubated with [α-^{32}P]-8-azido-ATP in the absence and presence of 5 mM $MgSO_4$ followed by ultraviolet irradiation. This led to the covalent incorporation of the ATP analogue into the recombinant proteins that was altered in the presence of $MgSO_4$ (Figure 2). Labeling of NBD1 (358−707) protein was enhanced approximately 4-fold in the presence of $MgSO_4$ (Figure 2A), whereas labeling of both NBD1 (358−590) and NBD1 (412−574) proteins was decreased in the presence of $MgSO_4$ (Figure 2B,C). Since labeling of full-length P-glycoprotein is enhanced in the presence of Mg^{2+}, it was assumed that NBD1 (358−707) may have retained ATP binding characteristics similar to those of the full-length protein but that the smaller proteins did not. Thus, additional experiments were performed with NBD1 (358−707) to further characterize the nature of ATP binding.

To determine if labeling of NBD1 (358−707) with [α-^{32}P]-8-azido-ATP could be saturated, protein was incubated with [α-^{32}P]-8-azido-ATP in the presence of 5 mM $MgSO_4$ and increasing concentrations (0.005−5 mM) of unlabeled 8-azido-ATP. Figure 3A depicts the quantitative representation of autoradiographic analysis from these experiments. These results demonstrate that labeling of NBD1 (358−707) was inhibited by 8-azido-ATP in a concentration-dependent manner with a half-maximal inhibition at 0.049 ± 0.011 mM. In a similar experiment, NBD1 (358−707) was incubated with [α-^{32}P]-8-azido-ATP in the presence of 5 mM $MgSO_4$ and increasing concentrations (0.005−5 mM) of ATP in order to evaluate if [α-^{32}P]-8-azido-ATP could be competed by the natural substrate. Labeling of NBD1 (358−707) was inhibited by ATP in a concentration-dependent manner with a half-maximal inhibition at 0.516 ± 0.111 mM (Figure 3B). These data indicate that [α-^{32}P]-8-azido-ATP labeling of NBD1 (358−707) protein is saturable and can be competed by ATP.

The specificity of [α-^{32}P]-8-azido-ATP labeling of NBD1 (358−707) protein was examined by incubating the protein in the presence of various hydrolyzable nucleotide analogues (1 mM). As shown in Figure 3C, ATP and GTP were able to inhibit labeling by 61% and 28%, respectively; UTP or CTP had no effect on labeling. At nucleotide concentrations

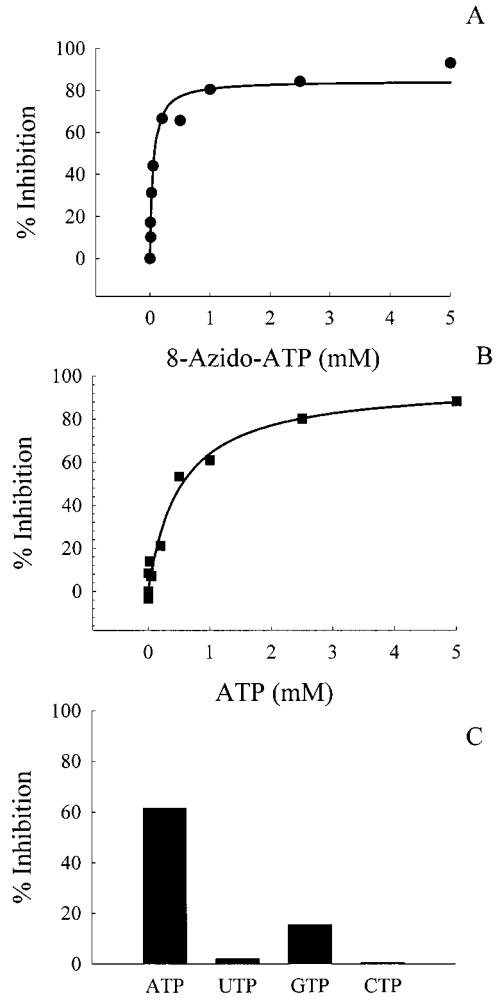

FIGURE 3: Specificity of [α-^{32}P]-8-azido-ATP labeling of NBD1 (358−707) protein. Protein was photoaffinity-labeled with 2.5 μM [α-^{32}P]-8-azido-ATP in the presence of 5 mM $MgSO_4$ and analyzed by SDS−PAGE and autoradiography. The percentage decrease in [α-^{32}P]-8-azido-ATP of NBD1 (358−707) protein vs (A) increasing concentrations of unlabeled 8-azido-ATP, (B) increasing concentrations of ATP, and (C) 1 mM concentrations of various nucleotide analogues. The line represents fit of the Michaelis−Menten model to the data by nonlinear least-squares regression analysis.

< 1 mM, only ATP was able to inhibit labeling to an appreciable extent; only at excessively high nucleotide concentrations (5 mM) were the other nucleotides able to inhibit ≥50% (data not shown). These results demonstrate that NBD1 (358−707) protein retains the ability to bind ATP with specificity similar to that of full-length P-glycoprotein.

D555N Amino Acid Substitution in the Walker B Consensus Sequence Results in an Alteration in Mg^{2+}-Enhanced ATP Binding. To evaluate the effect of Mg^{2+} on [α-^{32}P]-8-azido-ATP labeling, the NBD1 (358−707) protein was mutated at position 555 from aspartate to asparagine in the Walker B consensus motif (*36*). This mutation inhibits ATP binding and ATPase activity of full-length P-glycoprotein (*25*). Thus, the NBD1 D555N (358−707) protein serves as a specificity control in the present work. Expression and purification of NBD1 D555N (358−707) protein is shown in Figure 1. As demonstrated, NBD1 D555N (358−707) protein was localized in the inclusion-body protein and was purified by the methods described previously. Unlike the wild-type NBD1 (358−707) protein, [α-^{32}P]-8-azido-ATP labeling of the mutant NBD1 D555N (358−707) protein was greater in the absence of $MgSO_4$ than in the presence of $MgSO_4$ (Figure 2D). In fact, in the presence of $MgSO_4$ the ability of [α-^{32}P]-8-azido-ATP to label NBD1 D555N (358−707) protein was impaired severely (Figure 2D). Incubation of [α-^{32}P]-8-azido-ATP with NBD1 (358−707) protein or NBD1 D555N (358−707) protein in the presence of increasing concentrations of $MgSO_4$ resulted in an increase in labeling with wild-type protein and a decrease in labeling with mutant protein (data not shown). The specificity of labeling of NBD1 D555N (358−707) protein was explored by incubating the protein with [α-^{32}P]-8-azido-ATP in the presence of increasing concentrations of ATP in the absence of $MgSO_4$. Labeling of mutant protein in the absence of $MgSO_4$ appeared to be nonspecific since millimolar concentrations of ATP were required to achieve half-maximal inhibition (4.52 ± 0.16 mM) and ATP did not inhibit labeling at concentrations ≤ 1 mM (data not shown). These results demonstrate that $MgSO_4$ at concentrations ≥ 1 mM enhances the ability of 8-azido-ATP to interact with wild-type NBD1 (358−707) protein and that the aspartate residue in the Walker B motif plays a role in this interaction.

Analysis of NBD1 (358−707) and NBD1 D555N (358−707) proteins by CD was performed in order to assess the secondary structural components and to evaluate the effect of Mg^{2+}. The predicted secondary structural components of these proteins were 25% α-helix, 23% β-strand, and 19% β-turn; no differences between NBD1 (358−707) and NBD1 D555N (358−707) proteins were demonstrated (data not shown). Similarly, the predicted secondary structural elements of NBD1 (358−707) and NBD1 D555N (358−707) proteins in the presence of 2 mM $MgSO_4$ were not different than in the absence of $MgSO_4$ (data not shown). A temperature melt was performed to determine the thermal stability of NBD1 (358−707) and NBD1 D555N (358−707) proteins. Both proteins demonstrated 50% denaturation at ∼45 °C.

Minimal Unit of the Amino-Terminal Cytoplasmic Loop of Human P-Glycoprotein Required To Bind ATP Consists of the Amino Acid Region 375−635. We wanted to investigate the maximum length of the cytoplasmic loop required to retain Mg^{2+}-enhanced ATP binding. A series of plasmids, as shown in Table 1, were designed to express recombinant proteins with the results obtained from the earlier proteins as a basis for selection of the expressed sequences. Expression and purification of each protein is shown in Figure 4. One protein with a 17 amino acid deletion on the N-terminal end, NBD1 (375−707), retained the ability to incorporate [α-^{32}P]-8-azido-ATP in a Mg^{2+}-enhanced manner similar to NBD1 (358−707) (Figure 5). A protein with a 34 amino acid deletion on the N-terminal end, NBD1 (392−707), had a [α-^{32}P]-8-azido-ATP labeling ratio < 1.0, indicating that labeling was greater in the absence of Mg^{2+} than in the presence of Mg^{2+} (Figure 5). A protein with an intact N-terminal end and a 72 amino acid deletion on the C-terminal end, NBD1 (358−635) demonstrated enhanced labeling in the presence of magnesium, more than 3-fold greater than that of the intact NBD1 (358−707) protein (Figure 5). NBD1 (358−590) protein had an additional 45 amino acid deletion on the C-terminal end that abolished Mg^{2+}-enhanced [α-^{32}P]-8-azido-ATP labeling (Figure 5). A protein, NBD1 (348−635), with a 10 amino acid extension on the N-terminal end and a 72 amino acid deletion on the C-terminal end showed Mg^{2+}-enhanced labeling that was

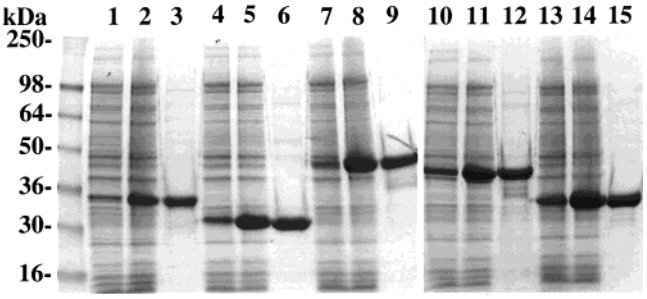

FIGURE 4: Expression and purification of NBD1 proteins. Protein fractions (10 μg of total protein per lane) were separated by SDS−PAGE and identified by colloidal blue staining (Novex, San Diego, CA). Expression of NBD1 proteins before (lanes 1, 4, 7, 10, and 13) and after (lanes 2, 5, 8, 11, and 14) IPTG induction. NBD1 proteins were as follows: NBD1 (358−635), lanes 1−3; NBD1 (409−635), lanes 4−6; NBD1 (375−707), lanes 7−9; NBD1 (392−707), lanes 10−12; and NBD1 (348−635), lanes 13−15. Purified NBD1 proteins were identified by colloidal blue staining as follows: NBD1 (358−635), lane 3; NBD1 (409−635), lane 6; NBD1 (375−707), lane 9; NBD1 (392−707), lane 12; and NBD1 (348−635), lane 15.

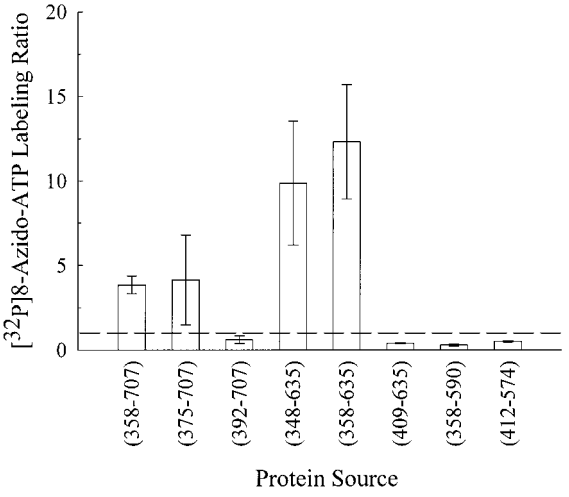

FIGURE 5: [α-^{32}P]-8-Azido-ATP labeling ratios of NBD1 proteins. NBD1 proteins (~100 pmol each) were labeled with 2.5 μM [α-^{32}P]-8-azido-ATP in the absence and presence of 5 mM $MgSO_4$ and analyzed by SDS−PAGE and autoradiography. Data represent the mean ratio of labeling in the presence and the absence of $MgSO_4$ ± SE (n = 3−13). Dashed line represents a ratio of 1.

greater than NBD1 (358−707) (Figure 5). Proteins with deletions on both N- and C-terminal ends that were after amino acid 375 and before amino acid 635 lost the ability to incorporate [α-^{32}P]-8-azido-ATP in a Mg^{2+}enhanced manner (Figure 5). These data show that a fragment of P-glycoprotein limited by amino acids 375−392 on the N-terminal end and amino acids 590−635 on the C-terminal end is required for Mg^{2+}-enhanced ATP binding but that the best binding is obtained with NBD1 (348−635) and NBD1 (358−635) proteins.

To determine if Mg^{2+}-enhanced [α-^{32}P]-8-azido-ATP labeling of NBD1 proteins was due to nonspecific interactions, proteins were heated to 100 °C for 5 min prior to incubation with [α-^{32}P]-8-azido-ATP. After heating, the protein solution was centrifuged to remove any aggregates and the supernatant was used in labeling experiments. Approximately 70% of the protein remained in the supernatant as determined by the Coomassie protein assay (Pierce, Rockford, Il.). Under these conditions labeling was reduced greatly after heat denaturation compared to undenatured protein, confirming that a proper conformation of the protein is required for labeling (data not shown).

Table 2: Kinetics of [α-^{32}P]-8-Azido-ATP Labeling Inhibition by ATP to NBD1 Proteins Derived from Human P-Glycoprotein

protein	IC_{50}[a] (μM)	% maximum inhibition
NBD1 (358−707)	566 ± 48.2	97.4 ± 1.8
NBD1 (375−707)	399 ± 29.9	97.6 ± 1.9
NBD1 (348−635)	180 ± 50.5	95.5 ± 4.1
NBD1 (358−635)	263 ± 90.7	102.2 ± 8.3

[a] Concentration at half-maximal inhibition.

Table 3: Kinetics of Mg^{2+}-Enhanced [α-^{32}P]-8-Azido-ATP Labeling of NBD1 Proteins Derived from Human P-Glycoprotein

protein	E_{max}[a] (arbitrary area)	EC_{50}[b] (μM)	γ[c]
NBD1 (358−707)	662 ± 18.9	723 ± 37.7	5.82 ± 0.85
NBD1 (375−707)	611 ± 14.2	411 ± 17.6	4.63 ± 0.73
NBD1 (348−635)	2056 ± 51.7	200 ± 12.6	4.33 ± 1.01
NBD1 (358−635)	1733 ± 171	466 ± 103	1.91 ± 0.72

[a] Area at maximal labeling. [b] Concentration at half-maximal labeling. [c] Degree of sigmoidicity.

To further evaluate nucleotide interaction with NBD1 recombinant proteins, the ability of the natural substrate ATP to inhibit [α-^{32}P]-8-azido-ATP labeling was compared among the NBD1 proteins. Each NBD1 protein at equivalent molar concentrations was incubated separately with 2.5 μM [α-^{32}P]-8-azido-ATP in the presence of 5 mM $MgSO_4$ and increasing concentrations (0.1−5 mM) of ATP. The NBD1 proteins that demonstrated Mg^{2+}-enhanced labeling [NBD1 (358−707), NBD1 (375−707), NBD1 (348−635), and NBD1 (358−635)], were inhibited by ATP in a concentration-dependent manner. Kinetic evaluation of the data revealed that each of these proteins was inhibited completely by ATP and that the apparent affinity of these protein for ATP was different (Table 2). Both of the smaller proteins, NBD1 (348−635) and NBD1 (358−635), had a 2−3-fold greater affinity for ATP than the larger proteins ending at position 707 (Table 2). These data suggest that the linker region (amino acids 635−707) may interfere with proper folding of the recombinant fragment, thus decreasing the affinity and capacity of ATP binding in these proteins. In contrast, proteins that did not demonstrate Mg^{2+}-enhanced labeling [NBD1 (392−707), NBD1 (409−635), NBD1 (358−590), and NBD1 (412−574)] were not inhibited by ATP in a specific manner. Labeling of any of these proteins was not inhibited at 0.5 mM ATP and was inhibited only marginally (<30%) at high ATP concentrations (5 mM).

To assess the influence of Mg^{2+} on the kinetics of [α-^{32}P]-8-azido-ATP labeling of NBD1 proteins that exhibit Mg^{2+}-enhanced labeling characteristics, NBD1 proteins of equivalent molar concentrations were incubated separately with 2.5 μM [α-^{32}P]-8-azido-ATP in the presence of increasing concentrations of $MgSO_4$. Each protein demonstrated enhanced labeling with increasing concentrations of $MgSO_4$ that was described well by the sigmoidal E_{max} model. Both of the smaller proteins, NBD1 (348−635) and NBD1 (358−635), incorporated [α-^{32}P]-8-azido-ATP approximately 3-fold more than the larger proteins (Table 3). Interestingly, the EC_{50} of [α-^{32}P]-8-azido-ATP labeling of NBD1 (348−635) was more

than 2-fold lower than any of the other NBD1 proteins evaluated, suggesting this fragment is more sensitive to magnesium (Table 3).

The nature of NBD1 (358−707), NBD1 (375−707), NBD1 (358−635), and NBD1 (348−635) proteins obtained by renaturation after guanidine solubilization was determined by size-exclusion chromatography as described under Experimental Procedures. The predicted molecular weight of each protein based on elution from the gel-filtration column was approximately equal to the theoretical molecular weight or slightly smaller, suggesting that the proteins eluted as apparent monomer species (data not shown).

In addition to evaluating the binding properties of the NBD1 proteins, we quantitated the recovery of the various proteins from renaturation to purification. The lowest recovery was observed for NBD1 (358−707) protein, where only 7% of the protein was accounted for at the end of the purification scheme. Comparatively, the recovery of NBD1 (375−707) protein and NBD1 (358−635) protein was higher with 22% and 43% recovered, respectively. The best recovery, 72%, was obtained for NBD1 (348−635) protein.

DISCUSSION

A major question concerning P-glycoprotein has been how this protein binds ATP and harnesses the energy from hydrolysis in order to function. The complexity associated with purifying and crystallizing membrane proteins has delayed the structural elucidation of ABC transporters of this type. An alternative approach to understanding the structural and functional characteristics of ABC transporters has involved the cloning of soluble recombinant protein domains that include NBD regions of these proteins. Previously, recombinant P-glycoprotein domains including NBDs from either the carboxyl- or amino-terminal half of mouse, Chinese hamster ovary, or human P-glycoprotein were reported (*11*−*16*); however, nucleotide binding properties in these studies were defined primarily by utilization of fluorescence-based analysis. Comparison of data obtained from fluorescence assays with soluble recombinant protein to that of the full-length protein may be compromised by interference from lipids necessary for stable reconstitution of the full-length protein. The aim of the present work was to design a soluble protein encompassing the N-terminal NBD from human P-glycoprotein that retained nucleotide-binding interactions similar to the full-length protein as determined by photoaffinity labeling studies with [α-^{32}P]-8-azido-ATP as the probe.

In the present work, human P-glycoprotein cDNAs with a C431A mutation were utilized to express a series of recombinant proteins containing NBD1 in *E. coli*. Expressed proteins were purified from inclusion bodies under denaturing conditions and renatured by rapid dilution. Previously, Loo and Clarke (*37*) demonstrated that mutation of cysteine residues to alanine did not alter the ability of P-glycoprotein to confer drug resistance and did not alter the characteristics of verapamil stimulation of ATPase activity. Therefore, this mutation was made in the present work to prevent disulfide interactions that may have hindered solubilization, renaturation, and purification. The initial protein domains chosen for expression were selected on the basis of the criteria that the expressed sequences must (1) contain the consensus Walker ATP binding motifs, (2) be derived from the sequence whose limits fall on the borders of predicted domains of defined secondary structure, (3) contain as many regions of high homology with other multidrug resistance proteins as possible, and (4) allow for detection of the expressed peptides by immunoblotting (e.g., sequences should contain the epitope recognized by the C219 monoclonal antibody, amino acids 569−574). Although the general premise was that shorter polypeptide chains may provide easier expression and facilitate subsequent structural analysis, a longer polypeptide was thought to provide a higher probability of obtaining a protein that would form a tertiary structure analogous to the native structure of this fragment. Thus, three proteins composed of the largest predicted fragment (amino acids 358−707) and two smaller fragments (amino acids 358−590 and 412−574) were chosen for expression and detailed analysis.

Characterization of the ATP-binding properties of the three NBD1 proteins with the photoactive ATP analogue [α-^{32}P]-8-azido-ATP revealed that only the NBD1 (358−707) protein retained the ability to bind ATP in a specific manner. Labeling of NBD1 (358−707) by [α-^{32}P]-8-azido-ATP was saturable and was inhibited by ATP and to a lesser extent by GTP, UTP, and CTP. More importantly, analysis of ATP binding by this technique enabled the demonstration of Mg^{2+}-enhanced ATP binding. Labeling of P-glycoprotein by [α-^{32}P]-8-azido-ATP was shown previously to be magnesium-dependent (*25*,*38*). Prior to the present investigation, the role of Mg^{2+} in ATP binding by recombinant NBD proteins of P-glycoprotein had not been explored.

The role of Mg^{2+}-enhanced ATP binding was evaluated by mutation of aspartate 555 located in the Walker B motif. This amino acid, well conserved within the consensus Walker B motif of ABC transporters and thought to play a role in binding the Mg^{2+} of the MgATP complex (*21*, *39*), was changed to asparagine to eliminate the ability to complex and stabilize ATP in the active site. In the present study, nonspecific labeling of mutant NBD1 (358−707) protein by [α-^{32}P]-8-azido-ATP was decreased in the presence of Mg^{2+}, suggesting that this residue confers Mg^{2+} dependence on ATP binding.

Secondary structural analysis of NBD1 (358−707) and NBD1 D555N (358−707) proteins by circular dichroism showed 25% α-helix, 23% β-strand, and 19% β-turn with no significant difference in secondary structure between the two proteins. Interestingly, the amino-terminal NBD protein from human CFTR displayed nearly identical proportions of secondary structural components as the NBD1 (358−707) proteins (*40*). Together these findings suggest that the amino-terminal NBD of various ABC proteins may be composed of similar secondary structural components. The secondary structural components of the carboxyl-terminal NBD protein from Chinese hamster ovary P-glycoprotein were 14% α-helix, 42% β-strand, and 20% β-turn (*13*), suggesting either that the carboxyl-terminal NBD has a somewhat different structure or that the fragments used in these studies were different. More interesting was the lack of secondary structural change of NBD1 (358−707) and NBD1 D555N (358−707) proteins in the presence of Mg^{2+}. These data are consistent with the hypothesis that the role of Mg^{2+} on ATP binding may involve a change in a higher ordered protein structure and not simply an alteration in secondary structural components.

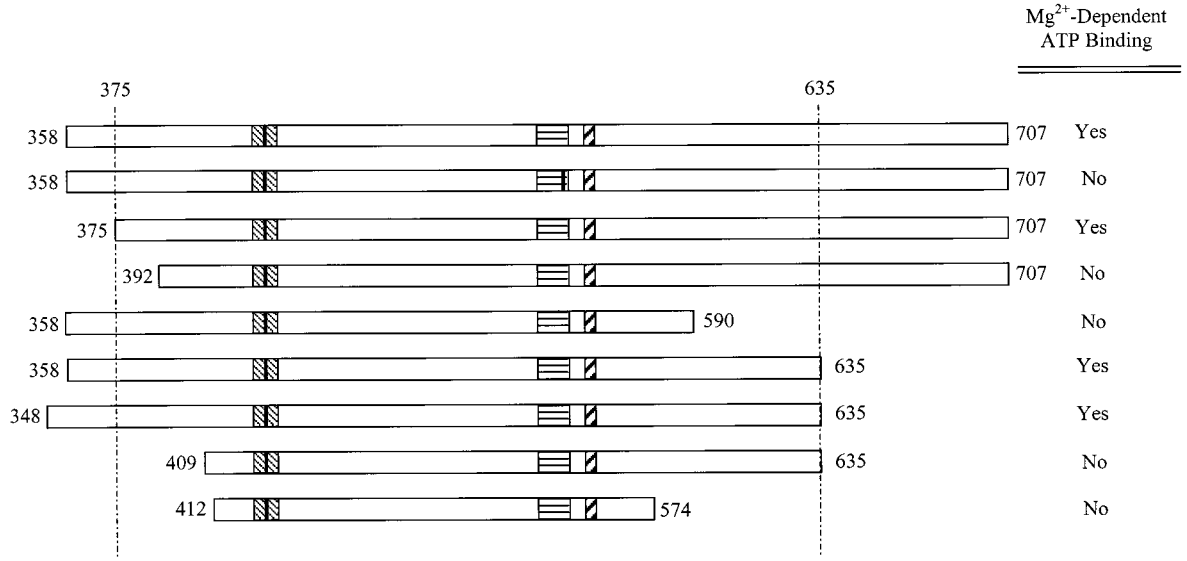

FIGURE 6: Summary of Mg^{2+}-dependent ATP binding of NBD1 recombinant protein constructs. Each rectangle represents a separate NBD1 protein with the N-terminal and C-terminal amino acid borders corresponding to the full-length P-glycoprotein indicated before and after the rectangle, respectively. The minimal unit required to retain Mg^{2+}-dependent [α-^{32}P]-8-azido-ATP labeling is indicated by the sequence within the dashed lines. The Walker motifs are indicated as follows: A, light hatched boxes; B, bold hatched boxes; and C, horizontally striped boxes. The C431A and D555N mutations within the Walker A and Walker B motifs, respectively, are identified by vertical bars.

To define the minimal functional unit required for specific ATP-binding, additional expression vectors were constructed. A series of plasmids were designed to express recombinant proteins with the results obtained from the initial proteins as a basis for selection of the expressed sequences. Since [α-^{32}P]-8-azido-ATP labeling of NBD1 (358−590) protein was not enhanced in the presence of $MgSO_4$, it was hypothesized that some of the amino acids between 590 and 707 may be required for Mg^{2+}-enhanced ATP binding or stabilization of the protein structure. It could not be speculated, on the basis of the data, if NBD1 (412−574) did not retain Mg^{2+}-enhanced ATP binding due to the loss of N-terminal amino acids or C-terminal amino acids; however, it was noted that this protein was approximately 10-fold more soluble and recovery was improved 10-fold over both NBD1 (358−707) and NBD1 (358−590) proteins. Thus, we investigated additional proteins that were altered on both the N- and C-terminal ends compared to NBD1 (358−707).

[α-^{32}P]-8-Azido-ATP labeling of NBD1 proteins of varying lengths identified the region between amino acids 375−392 and 590−635 as the region necessary to obtain specific ATP binding (Figure 6). Recombinant NBD1 proteins not conforming to this region demonstrated nonspecific [α-^{32}P]-8-azido-ATP labeling. This observation is consistent with previously published data, where an NBD1 protein from mouse P-glycoprotein comprising of amino acids 395−581 required more than 6 mM ATP to inhibit TNP-ATP binding, and [α-^{32}P]-8-azido-ATP labeling in the presence of magnesium only was partially inhibited in the presence of 8 mM ATP (*14*).

Comparison of the kinetics of ATP binding and the effect of magnesium on ATP binding determined in this work to that previously published for the full-length protein (*25*) suggests that NBD1 (348−635) retains the ability to bind ATP in a similar manner. The concentration of magnesium required to obtain half-maximal [α-^{32}P]-8-azido-ATP incorporation was 200 ± 12.6 μM for the recombinant protein in this study compared to 153 ± 29.9 μM for the full-length protein (*25*). The concentration of ATP required to inhibit [α-^{32}P]-8-azido-ATP labeling by 50% was about 10-fold higher with the recombinant protein compared to the full-length protein (180 ± 50.5 μM vs 12.8 ± 4.2 μM, respectively) suggesting that the affinity of ATP for the recombinant protein was less. This is most likely due to a loss in protein stability that resulted from the lack of transmembrane domains or the involvement of the C-terminal nucleotide-binding domain in ATP binding.

P-Glycoprotein has been shown to have readily detectable basal ATPase activity that can be stimulated 2−10-fold in the presence of certain substrates (e.g., verapamil) (*5*). The ATPase activity of the recombinant proteins described in this work was negligible under these conditions. These results are consistent with those observed for other recombinant NBD proteins of P-glycoprotein where ATPase activity was negligible or more than 10-fold lower than the full-length protein (*13*, *14*, *16*). The lack of appreciable ATPase activity with soluble NBD proteins supports the hypothesis that ATPase activity of P-glycoprotein may require both functional NBDs (*13*, *25*), and/or NBDs may not be able to hydrolyze ATP in the absence of membrane binding components (*41*), with or without endogenous substrates.

In summary, the present study demonstrates that NBD1 proteins containing the amino acid region 375−392 through 590−635 retain the ability to bind ATP in a specific Mg^{2+}-dependent manner. Although the present data suggest that a minimal functional unit is required for specific ATP binding, the differences seen in the ATP-binding properties of the various recombinant NBD1 proteins also may be the result of differences in the renaturation properties of these proteins. The NBD1 (348−635) protein may be of particular interest in future structural evaluation because its nucleotide binding properties most closely resemble that of the membrane-bound form of the full-length protein and it can be produced in good yield.

ACKNOWLEDGMENT

We like to thank Dr. Andrea Keppler-Hafkemeyer (LMB, NCI, NIH) for guidance with protein expression and purification, Dr. Christine A. Hrycyna (LCB, NCI, NIH) for help with expression vector construction and photoaffinity labeling, and Dr. Garrot W. Christoph (LCP, NIDDK, NIH) for assistance with CD analysis.

REFERENCES

1. Fojo, A. T., Ueda, K., Slamon, D. J., Poplack, D. G., Gottesman, M. M., and Pastan, I. (1987) *Proc. Natl. Acad. Sci. U.S.A. 84*, 265−269.
2. Thiebaut, F., Tsuruo, T., Hamada, H., Gottesman, M. M., Pastan, I., and Willingham, M. C. (1987) *Proc. Natl. Acad. Sci. U.S.A. 84*, 7735−7738.
3. Gottesman, M. M., and Pastan, I. (1988) *J. Biol. Chem. 263*, 12163−12166.
4. Horio, M., Gottesman, M. M., and Pastan, I. (1988) *Proc. Natl. Acad. Sci. U.S.A. 85*, 3580−3584.
5. Ambudkar, S. V., Lelong, I. H., Zhang, J., Cardarelli, C. O., Gottesman, M. M., and Pastan, I. (1992) *Proc. Natl. Acad. Sci. U.S.A. 89*, 8472−8476.
6. Ko, Y. H., and Pederson, P. L. (1998) *Methods Enzymol. 292*, 675−686.
7. Nikaido, K., Liu, P. Q., and Ames, G. F. (1997) *J. Biol. Chem. 272*, 27745−27752.
8. Gallagher, M. P., Pearce, S. R., and Higging, C. F. (1989) *Eur. J. Biochem. 180*, 133−141.
9. Capieaux, E., Rapin, C., Thines, D., Dupont, Y., and Goffeau, A. (1993) *J. Biol. Chem. 268*, 21895−21900.
10. Falson, P., Penin, F., Divita, G., Lavergne, J.-P., Di Pietro, A., Goody, R. S., and Gautheron, D. C. (1993) *Biochemistry 32*, 10387−10397.
11. Conseil, G., Baubichon-Cortay, H., Dayan, G., Jault, J.-M., Barron, D., and Di Pietro, A. (1998) *Proc. Natl. Sci. Acad. U.S.A. 95*, 9831−9836.
12. Baubichon-Cortay, H., Baggetto, L. G., Dayan, G., and Di Pietro, A. (1994) *J. Biol. Chem. 269*, 22983−22989.
13. Sharma, S., and Rose, D. R. (1995) *J. Biol. Chem. 270*, 14085−14093.
14. Dayan, G., Baubichon-Cortay, H., Jault, J.-M., Cortay, J.-C., Deleage, G., and Di Pietro, A. (1996) *J. Biol. Chem. 271*, 11652−11658.
15. Dayan, G., Jault, J.-M., Baubichon-Cortay, H., Baggetto, L. G., Renoir, J.-M., Baulieu, E.-E., Gros, P., and Di Pietro, A. (1997) *Biochemistry 36*, 15208−15215.
16. Wang, C., Castro, A. F., Wilkes, D. M., and Altenberg, A. (1999) *Biochem. J. 338*, 77−81.
17. Cheng, K., and Koland, J. G. (1996) *J. Biol. Chem. 271*, 311−318.
18. Moutin, M.-J., Cuillel, M., Rapin, C., Miras, R., Anger, M., Lompré, A.-M., and Dupont, Y. (1994) *J. Biol. Chem. 269*, 11147−11154.
19. Rossi, F., Labourier, E., Gallouzi, I. E., Derancourt, J., Allemand, E., Divita, G., and Tazi, J. (1998) *Nucleic Acids Res. 26*, 2963−2970.
20. Bandorowicz-Pikula, J., and Awasthi, Y. C. (1997) *FEBS Lett. 409*, 300−306.
21. Ueda, K., Inagaki, N., and Seino, S. (1997) *J. Biol. Chem. 272*, 22983−22986.
22. Schafer, H. J. (1986) *Methods Enzymol. 126*, 649−660.
23. Rieger, T., Napiwotzki, J., Huther, F. J., and Kadenbach, B. (1995) *Biochem Biophys. Res. Commun. 217*, 34−40.
24. Cornwell, M. M., Tsuruo, T., Gottesman, M., and Pastan, I. (1987) *FASEB J. 1*, 51−54.
25. Hrycyna, C. A., Ramachandra, M., Germann, U. A., Wu, P., Pastan, I., and Gottesman, M. M. (2000) *Biochemistry* (in press).
26. Soultanas, P., Dillingham, M. S., Velankar, S. S., and Wigley, D. B. (1999) *J. Mol. Biol. 290*, 137−148.
27. Zhou, T., and Rosen, B. P. (1999) *J. Biol. Chem. 274*, 13854−13858.
28. Weber, J., Hammond, S. T., Wilke-Mounts, S., and Senior, A. E. (1998) *Biochemistry 37*, 608−614.
29. Ramachandra, M., Ambudkar, S. V., Gottesmann, M. M., Pastan, I., and Hrycyna, C. A. (1996) *Mol. Biol. Cell 7*, 1485−1498.
30. Brinkmann, U., Lee, B. K., and Pastan, I. (1993) *J. Immunol. 150*, 2774−2782.
31. Laemmli, U. K. (1970) *Nature 227*, 680−685.
32. Ramachandra, M., Ambudkar, S. V., Chen, D., Hrycyna, C. A., Dey, S., Gottesman, M. M., and Pastan, I. (1998) *Biochemistry 37*, 5010−5019.
33. Sarkadi, B., Price, E. M., Boucher, R. C., Germann, U. A., and Scarborough, G. A. (1992) *J. Biol. Chem. 267*, 4854−4858.
34. Shepard R. L., Winter,, M. A., Hsaio, S. C., Pearce, H. L., Beck, W. T., and Dantzig, A. H. (1998) *Biochem. Pharmacol. 56*, 719−727.
35. Al-Shawi, M. K., Urbatsch, I. L., and Senior, A. E. (1994) *J. Biol. Chem. 269*, 8986−8992.
36. Walker, J. E., Saraste, M., Runswick, M. J., and Gay, N. J. (1982) *EMBO J. 1*, 945−951.
37. Loo, T. W., and Clarke, D. M. (1995) *J. Biol. Chem. 270*, 843−848.
38. Hrycyna, C. A., Airan, L. E., Germann, U. A., Ambudkar, S. V., Pastan, I., and Gottesman, M. M. (1998) *Biochemistry 37*, 13660−13673.
39. Schulz, G. E. (1992) *Curr. Opin. Struct. Biol. 2*, 61−67.
40. Neville, D. C. A., Rozanas, C. R., Tulk, B. M., Townsend, R. R., and Verkman, A. S. (1998) *Biochemistry 37*, 2401−2409.
41. Mimmack, M. L., Gallagher, M. P., Pearce, S. R., Hyde, S. C., Booth, I. R., and Higgins, C. F. (1989) *Proc. Natl. Acad. Sci. U.S.A. 86*, 8257−8261.

BI992931X